water

MDPI

Article

Soil Erosion Assessment Using the RUSLE Model and Geospatial Techniques (Remote Sensing and GIS) in South-Central Niger (Maradi Region)

Mohamed Adou Sidi Almouctar [1,2], Yiping Wu [1,2,*], Fubo Zhao [1,2] and Jacqueline Fifame Dossou [1]

[1] Technology Innovation Center for Land Engineering and Human Settlements, Shaanxi Land Engineering Construction Group Co., Ltd., Xi'an Jiaotong University, Xi'an 710049, China; sidialmoctarp@gmail.com (M.A.S.A.); zfubo789@163.com (F.Z.); dofiline@yahoo.fr (J.F.D.)

[2] Department of Earth and Environmental Science, School of Human Settlements and Civil Engineering, Xi'an Jiaotong University, Xi'an 710049, China

* Correspondence: yipingwu@xjtu.edu.cn; Tel.: +86-186-8182-6576

Abstract: A systematic method, incorporating the revised universal soil loss equation model (RUSLE), remote sensing, and the geographic information system (GIS), was used to estimate soil erosion potential and potential area in the Maradi region of south-central Niger. The spatial trend of seasonal soil erosion was obtained by integrating remote sensing environmental variables into a grid-based GIS method. RUSLE is the most commonly used method for estimating soil erosion, and its input variables, such as rainfall erosivity, soil erodibility, slope length and steepness, cover management, and conservation practices, vary greatly over space. These factors were calculated to determine their influence on average soil erosion in the region. An estimated potential mean annual soil loss of 472.4 t/ac/year, based on RUSLE, was determined for the study area. The potential erosion rates varied from 14.8 to 944.9 t/ac/year. The most eroded areas were identified in central and west-southern areas, with erosion rates ranging from 237.1 to 944.9 t/ac/year. The spatial erosion maps can serve as a useful reference for deriving land planning and management strategies and provide the opportunity to develop a decision plan for soil erosion prevention and control in south-central Niger.

Keywords: remote sensing; GIS technique; RUSLE model; soil erosion; land use change; climatic zones; Maradi region

Citation: Sidi Almouctar, M.A.; Wu, Y.; Zhao, F.; Dossou, J.F. Soil Erosion Assessment Using the RUSLE Model and Geospatial Techniques (Remote Sensing and GIS) in South-Central Niger (Maradi Region). *Water* **2021**, *13*, 3511. https://doi.org/10.3390/w13243511

Academic Editors: Mirko Castellini and František Petrovič

Received: 30 September 2021
Accepted: 1 December 2021
Published: 9 December 2021

1. Introduction

Soil erosion was known to be one of the most important environmental problems in the nineteenth and twentieth centuries, especially for developing country [1,2]. Soil erosion is one of the world's greatest scientific problems. It has various negative consequences, such as land degradation, decreasing water quality, sedimentation of rivers, and destruction of roads [3]. As well as these, it directly affects food production, human health, and the earth's environment. For example, the gradual degradation of habitat is mainly caused by extreme soil erosion [4,5]. Soil erosion is the detachment of soil and its movement and deposition by various methods [6]. The issue has far-reaching political, social, economic, and environmental consequences, as it causes damage, both on-site and off-site [7–10], in many countries [11,12]. Moreover, soil erosion leads to a decrease in soil fertility, which has become a threat to sustainable agricultural production and water quality in these regions [13,14]. Furthermore, surface water change is generally symbolic of global analysis variance in a research region, where hydrological process might better understand the natural and anthropogenic disruption of meteorological features, as well as projected trends in water management [15,16].

Erosion is the process of the detachment and transport of soil particles by erosion forces. These erosive forces can be wind, ice, or water in the form of raindrop action and

surface runoff [17]. On the other hand, erosion by wind, water, ice, or gravity can be defined as the removal of the earth's surface material. The hazards associated with extremely rapid erosion have existed for over a million geological years in most regions of the earth. Nevertheless, the problem has been exacerbated in recent times by increasing human influence on the environment. Furthermore, data collection on soil erosion is typically capital intensive and time-consuming [18,19]. In addition, the effects of soil erosion appear to pose a serious threat to human existence [20,21], As one element of soil degradation, it leads to the deterioration of soil's physical, chemical, and biophysical characteristics.

Furthermore, various research measures of soil erosion have been established, and it is a common opinion that the area affected by erosion can be the best predictor for soil erosion research [22]. Apart from this, soil erosion is the most serious type of land loss that threatens the food security and natural economy of regions, both locally and globally [23,24]. Soil erosion in catchment areas and on the banks of reservoirs and lakes leads to siltation. This may result in increased turbidity, clogging of hydraulic structures, and reduced safety for flood retention [23]. Thus, soil erosion caused by anthropogenic activity in the watershed is a key factor in reservoir sedimentation. The silt is carried downstream by rivers, which eventually lead to reservoirs. The geology, geographical character, climate, plant types, and land use within the drainage basin influence the amount and kind of sediment [24]. According to Kastridis and Kamperidou (2015) [25], the issue of land use is very important and can influence the erosion process in a positive or negative way. Vacca et al. (2000) compared runoff and soil erosion measurements from three hillslopes with varying land uses and concluded that land use has a significant impact on runoff and erosion rate [26]. Additionally, soil erosion is a dynamic phenomenon, with numerous, and various unknown, impacts on the lives of people and the environment [27]. Decreased soil fertility leads to the degradation of natural habitats, such as forests, pastures, and rural ecosystems. Soil erosion is an important index for the evaluation and sustainability of soil conservation strategies [28,29]. Nowadays, poor soil conditions in an area have a negative impact on vegetation development, making the water system and vegetation susceptible [16].

An appropriate model of soil erosion can be applied to measure the soil erosion levels of a specific region. Erosion simulation can be used as a statistical tool to measure soil degradation and soil erosion potential for environmental planning [21]. Therefore, soil erosion has economic and political importance, as well as social and environmental impacts [30]. Brath et al. (2002) [31] Used a regional application of RUSLE to analyze the impact of land use on erosion, based on information about terrain morphology atmosphere, soil, and land use. Several studies have assessed soil erosion losses in different regions of the world using remote sensing and GIS technology [32–35]. Their analyses showed that changes in land use seriously affected annual soil loss. On the other hand, some studies have attempted to quantitatively evaluate these changes and concluded that the human influence in driving changes in sediment output is more important than climate change [4].

Moreover, determining the economic value of soil erosion requires field knowledge. Many models have been developed to estimate soil loss, such as the universal soil loss equation (USLE) [36] and the revised universal soil loss equation (RUSLE) [37].Several researchers combined erosion models with remote sensing tools and geographic information systems (GIS) [38–40] to improve the accuracy of the erosion estimation and to predict spatial maps of soil erosion risk. Moreover, soil erosion is a natural process of soil material removal and transport due to the action of erosive agents such as water, wind, gravity, and human disturbance [41,42]. However, when soil erosion occurs faster because of human disturbance, it has negative ecological and economic impacts. Modelling for erosion in Niger is difficult, due to a lack of data, especially the data related to soils. Key parameters of erosion prediction models, such as soil erodibility, expressed as k-factor, are difficult to obtain [43,44]. While, wind and water erosion are commonly believed to be prevalent in the Sahel, there is no evidence of the rate of soil erosion or the impact on agriculture [43]. To remedy this, indirect approaches are used to estimate these factors to make these studies

feasible [45]. Seeking an appropriate model that can accurately measures soil loss from all types of erosion at a given site remains a challenge.

There are several soil erosion models, with varying degrees of complexity. One of the most widely used empirical models for assessing sheet and rill erosion is USLE, developed by Wischmeier and Smith in 1965. USLE was originally developed primarily for estimating soil erosion in cropland or gently sloping topography, and has revised (RUSLE) and modified (MUSLE) versions [46,47].

In this context, the satellite remote sensing can be a convenient way to solve the problem. Remote sensing (RS) provides data over vast regions, with the ability to visit the same land area regularly. Furthermore, it can make an important contribution to regional soil erosion risk assessment through the rapid derivation of appropriate indices [48–50]. GIS and remote sensing are widely applied in many research areas, mainly in flood risk assessment, which is directly associated with soil erosion, as extreme hydrological events generate soil erosion and sediment transport. According to Tzioutzios, 2020, by taking advantage of the advanced capabilities offered by GIS, this task can be expedited, so that results and decisions are less time consuming, more efficient, and more accurate [50]. The use of GIS and spatial data plays a leading role in this area; by applying simple spatial techniques to the datasets and combining them with the RUSLE model. GIS and RS allow the use of spatial data of different types. Confirming this, recently made available datasets and technologies (satellite data and GIS) provide an adequate spatial and temporal accuracy, which ultimately leads to better flood risk reduction [51].Additionally, there have been some published studies on the application of RS and GIS technologies for soil erosion modelling in other parts of the world [52], yet little or no work was found on the application of GIS for erosion modelling in south-central Niger (Maradi region).

Therefore, this study aimed to estimate soil erosion potential using RUSLE, RS, and GIS technology in south-central Niger. The specific aims were to: (a) create a method that integrates remote sensing data and GIS with the RUSLE to estimate the spatial distribution of soil erosion of the overall study area, (b) provide a complete map of soil erosion susceptibility and land use/cover changes using RS and GIS, and (c) identify the areas of high and low soil erosion in the study area using the overlay approach.

The spatial erosion maps produced using the RUSLE model, by combining RS and GIS technology, can serve as a useful input for deriving land planning and management strategies and provide an opportunity to develop a decision plan for soil erosion prevention and control in south-central Niger.

2. Materials and Methods

2.1. Description of the Study Area

The Maradi Region is situated between 13° and 15°26′ north latitude and 6°16′ and 8°36′ east longitude in the south-central part of Niger (Figure 1). It is located in central Niger between the Damagram and Ader-Doutchi Rivers, with dune soils (soils on dunes). The area is bordered by Zinder, Tahoua, Agadez, and the Federal Republic of Nigeria. The region covers 41,796 km^2, or 3.30 percent of the country. These are the land types: agriculture (71.5%), pasture (25%), and woodland (1.463) (3.5 percent).

Maradi has two different climate zones. The northern Sahelian Climate has an average annual rainfall of 200–300 mm. The southern regions have a Sahelian–Sudanese climate with 500–600 mm annual rainfall. It is dry and cold from October to February, with mean annual temperatures of −10 °C; dry and hot from March to May, with temperatures reaching 40 °C; and wet and chilly from June to September. This area also has a rainfall gradient that diminishes from south to north. The average annual rainfall for the previous ten years was 493.3 mm in the south (Madarunfa rainfall station) and 342.7 mm in the north (Fako rainfall station) [53].

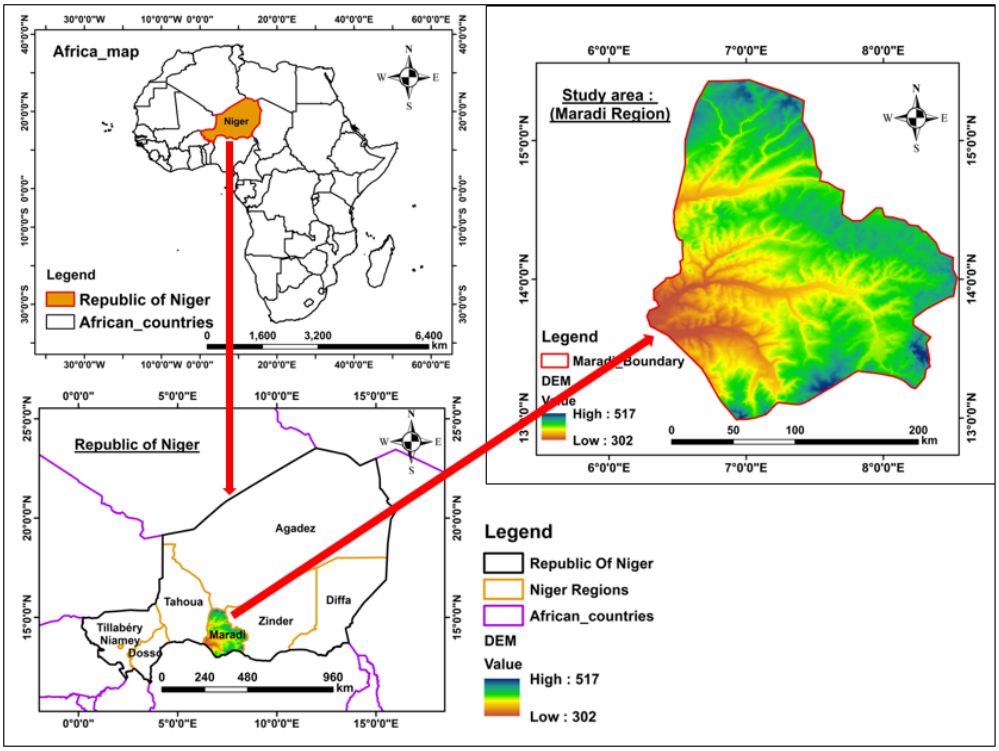

Figure 1. Location map of the study area.

2.2. Data Source Processing

RUSLE has been applied in a GIS approach in a variety of contexts, including mountainous tropical watersheds, large-scale watersheds, agriculturally dominant watersheds, areas with distinct wet and dry seasons, and areas with dynamic changes in land cover patterns, agricultural farmlands, and development. The RUSLE model is composed of three primary databases: (1) Climatic and survey database, including monthly temperature and precipitation data, as well as contours necessary for computing the erosivity factor, slope length, and steepness factors (LS). (2) The crop database stores data essential for calculating the surface cover factor (C). (3) The soil data set comprises soil survey and characterization information, which is used to calculate the soil erodibility factor (K).

The RUSLE model determines the yearly average loss of soil erosion, by taking into account the five elements indicated in Equation (1) [36].

$$A = R \times K \times LS \times C \times P \quad (1)$$

where A is the approximate average soil loss in tonnes per hectare per year (t ha^{-1} $year^{-1}$), R is the measure of rainfall erosivity factor expressed in (MJ·mm ha^{-1} h^{-1} $year^{-1}$), K is the soil erodibility index in (t·hr/MJ·mm), LS is the topographic factor = slope length and slope steepness factor (dimensionless), C is the cover management factor = cropping management factor (dimensionless), and P is the support measures/practice control factor (dimensionless).

The RUSLE approach is often used to estimate each element in the model. Previous scholars established a variety of methods for predicting these parameters, including the use of climatic data, soil and geological maps, remotely sensed satellite pictures, empirical formulae, and digital elevation models (DEM) derived from a variety of sources. The following parts of this article detail the procedures used to construct the model factors and the findings received.

Each of the factors was derived separately in raster data format, and erosion was determined using the algebra map function. The ArcGIS Spatial Analyst method (10.3) was used to delineate the boundary of the study area.

The RUSLE parameters were determined using a separate equation, whose input was obtained from satellite imagery and DEM. The inputs, their origin, and the equations used are listed in Table 1. Equations available in the literature for calculating the variables were iteratively reviewed and the best equations were selected based on their suitability for use with the available data and their ability to provide estimates comparable to the reported field-based erosion measurements. The estimation of each factor is discussed in more detail in the following sections, see Figure 2.

Table 1. Description of the data sources.

No	Type of Data	Data Description	Name of the Service That Provide the Data
1	DEM	SRTM DEM (30 s resolution) Grid format	DIVA-GIS Satellite [54]
2	Soil Data	FAO Digital soil Map of the World (DSMW)	Food and Agriculture Organization of the United Nations [55]
3	Satellite Data	MODIS/Tera Aqua Combined land cover type yearly global 500 m SIN Grid V006	National Aeronautics and Space Administration (NASA) [56]
5	Rainfall Data	TRMM is a mission between NASA and the Japan Aerospace Exploration Agency (JAXA)	NASA and the Japan Aerospace Exploration Agency (JAXA) [57]

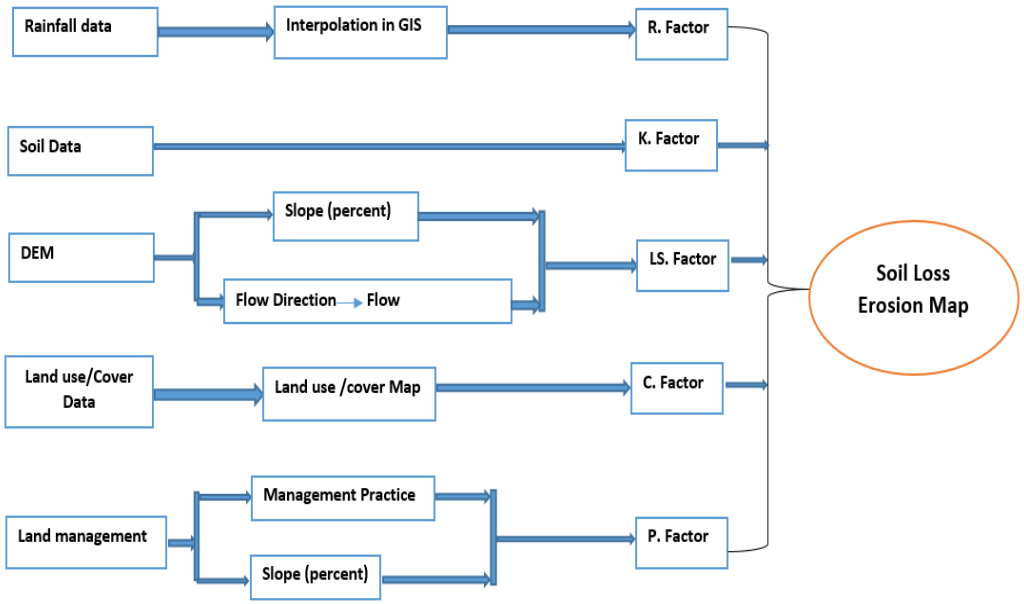

Figure 2. Flow chart for the analysis of soil loss based on the RUSLE model, remote sensing, and GIS technique.

Rainfall Erosivity (R factor): rainfall erosivity is the most important factor in RUSLE and responsible for soil erosion in an area. It is a long-term average of rainfall erosivity. Thus, the R-factor describes the intensity of precipitation in a given location, based on the extent of soil erosion [58,59], which is essential for assessing soil erosion risk under future land use and climate change [59]. The R factor quantifies the influence of precipitation on the amount and rate of runoff factor [50,51]. In the present analysis, the rainfall erosivity was calculated using the mean annual rainfall data collected from two monitoring stations in the Maradi region (Madarunfa rainfall station in the south of the region and Fako rainfall station in the north). In this section we used the Renard and Freimund (1994) equation, which establishes a relation between (R) and the average annual rainfall. Furthermore, it can be used for locations with a mean annual precipitation of less than 850 mm. The following formula was used to calculate the R factor:

$$R = 0.0483 \times P^{1.61} \quad (2)$$

where R is the measure of rainfall erosivity expressed in (MJ·mm ha^{-1} h^{-1} year^{-1}) in the RUSLE equation and P is the average annual precipitation (mm).

Soil Erodibility (K-factor): The K-factor reflects the susceptibility of the soil type to erosion, the transportability of sediments, and the amount and velocity of runoff for an appropriate rainfall input [32]. The soil maps of the region were prepared using FAO Digital Soil Map of the Word Shapefile (DSMW), where the zone of interest was captured over the respective area and the soil data layer was clipped to the study area in ArcGIS environment 10.3. The soil maps and K-factor values obtained from the literature for each soil type were then used to calculate the soil classes for the study area and then entered into ArcGIS and analyzed to obtain a K-factor map. The K-factor values (Table 2) for the corresponding soil groups were used in the analysis.

Table 2. K-factor value for soil erosion.

Code No	Soil Sample	Fao Soil Classes	K-Factor Values
1	Ql1-1a-1614	Luvic Arenosols	0.016
2	Re35-a-1686	Eutric Regosols	0.018
3	Ge5-1a-1211	Eutric Gleysols	0.019
4	Qc7-1a-1607	Arenosols	0.02
5	Lf40-1a-1467	Ferric Luvisols	0.021
6	I-Lf-Ql-1261	Lithosols	0.022
7	Lg20-1504	Gleyic Luvisols	0.027

The K-factor represents the sensitivity of a soil to the isolation and transfer of soil particles. It reflects the combined effect of the soil's properties and shows the general tendency for erosion of a particular soil type [29]. Soils that have different properties have different resistances to erosion. Erodibility, therefore, varies with the physical and biochemical properties of the soil, such as soil texture and structure, aggregate stability, shear strength, infiltration capacity for organic matter, and chemical content. The respective K-factor values for each soil type were assigned based on the existing soil types in the study area [60,61].

Slope length and steepness (LS-factor): slope factor and steepness (LS) are equivalent to topographic factor and relief factor, respectively. This factor is a combined factor of slope length and slope steepness. Furthermore, the slope length factor L calculates the erosion effect of slope length and the slope steepness factor S calculates the erosion effect of slope steepness. The parameters associated with topography were derived from the digital elevation model (DEM). To create the LS-factor map, flow direction and flow accumulation maps were processed after the filling process and created from DEM data in the GIS extension Arc Hydro Tools, to be used as input for the LS-factor calculation. To better understand this, the FA were obtained as flows, by calculating the flow direction with DEM. For each cell, the flow accumulation was determined by the flow that flows through that cell; if the flow accumulation value is greater, the area will form a runoff more easily. The LS values can be estimated as follows:

$$LS = \{FA \times (\text{cell size}/23.13)\}^{0.4} \times \{\text{Sin (slope of DEM} \times 0.01745)/0.09\}^{1.3} \times 1.6 \quad (3)$$

where LS: slope length and slope steepness factor; FA: flow accumulation

Land cover management (C-Factor): According to Molla et al. [29], the C-factor quantifies the cumulative effects on land degradation of trees, crop sequences, and other land cover areas, with values ranging from 0.01 to 1. The C-factor is dimensionless. Although C-factor values (Table 3) were used in this analysis. The C-factor maps were quantified from the land use/land cover groups of the reservoir catchments. To determine the C-factor it is necessary to rely, as much as possible, on current land use/land cover

data, which reflect the present status of the research area [17]. The C-factor is the most important factor in crop management and, perhaps, the most important factor in the RUSLE model, because it is the easiest aspect to manage for erosion mitigation. Although the corresponding proposed C-factor values for different land use/land cover groups were assigned based on the categorized map, these values were taken from previous studies and distributed among the respective land use/land cover forms. Finally, the C-factor map was created using the GIS database.

Table 3. C values for different LULC classes.

Gridcode No	LU/LC Types	Area	C-Values
7	Forest	7534.17	0.01
10	Shrublands	0.72	0.07
12	Barren	33.84	0.18
13	Grasslands	4663.8	0.23
14	Croplands	4237.47	0.28
16	Urban and Built-up	78.93	1

Conservation practice (P-factor): the ratio between the soil loss of a field with a particular conservation method and a field where no conservation is practiced is expressed by the P-factor. It is a measure of the success of land management practices in reducing soil degradation in an area [62,63]; because of the erosion capacity of runoff, by manipulating the runoff conditions, concentration, velocity, and hydraulic forces of runoff, the management activities reduce the rate of soil erosion [32]. Thus, all agricultural activities that can discourage or reduce soil erosion were considered in this review. For further processing, the MODIS MCD12Q1 images were categorized using the maximum probability classifier and the *p*-value pixels were assigned to each land use and land cover class.

2.3. Limitations and Uncertainties

This section discusses a few of the key limitations of our research methodology, including geographic applicability, model uncertainty, input data, and validation.

Many of the limitations and uncertainties in our research could be attributed to existing RUSLE formulations, including uncertainty associated with the model's simple empirical nature and numerous subcomponents; data availability issues; and the model's inability to account for soil loss due to gully erosion, mass sliding events, or the prediction of potential sediment yields in streams.

The RUSLE model ignores gully erosion. Identifying and measuring gullies in the watershed will improve the accuracy of soil loss estimation for future conservation practices, planning, and management. Determining the most sensitive input parameters that guide selective and targeted interventions was not carried out either [63]. Further research on the effect of soil loss on agricultural output and rural lives is needed to establish a relationship between soil loss and unsustainable soil management methods. The study may also not have fully appreciated the quantitative aspects of model outputs, due to subjective community perceptions. In order to make sound decisions, we need more evidence.

The limitations of the USLE make it seem as if we lack a properly informed understanding of the extent of soil erosion in our region, let alone the mechanisms of sediment transport and deposition [64]. Indeed, the validation of the main result of the study was accomplished via the use of the RUSLE model in conjunction with local perspectives. As input parameters, soil, land use/cover, DEM, rainfall, and support practice data were employed. The raster layers were processed to display the relevant input parameters on the ArcGIS platform, and the inputs were then multiplied to calculate the yearly average rate of soil loss and create intensity maps for the research area.

After completing data entry operations and organizing each information layer, the mean yearly soil loss was estimated by multiplying each component layer together according to the RUSLE formula (Equation (1)) in a GIS framework, utilizing the raster calculator of map algebra functions and accompanying packages [65].

3. Results and Discussion

3.1. Soil Loss Rate Assessment

In this study, we used remote sensing, GIS techniques, and the RUSLE model to estimate the extent and spatial distribution of soil erosion in the study area. Furthermore, five erosion risk factors were calculated, including rainfall erosivity (R-factor), soil erodibility (K-factor), slope duration and steepness (LS-factor), land cover management (C-factor), and soil protection/conservation practices (P-factor).

Rainfall erosivity (R-factor): the calculated R-factor (Figure 3b) ranged from 0.011 to 1644.6 MJ mm/h ha yr. The average rainfall erosivity of the study area was 822.3 MJ mm/h ha yr. It was observed that rainfall is high in the southern part of the study area, as indicated by the results. In addition, the erosivity value of rainfall shows that the R-value is greater in a regions where the rainfall quality and intensity is higher and vice versa. Therefore, the different distributions of rainfall within the study area cannot be satisfactorily explained by a single R-value [66,67]. However, it showed that rainfall erosivity is an important factor in assessing soil erosion for future land-use/land-cover and climate change. Thus, this is due to changes in climate, interannual rainfall distribution, and rainfall intensity.

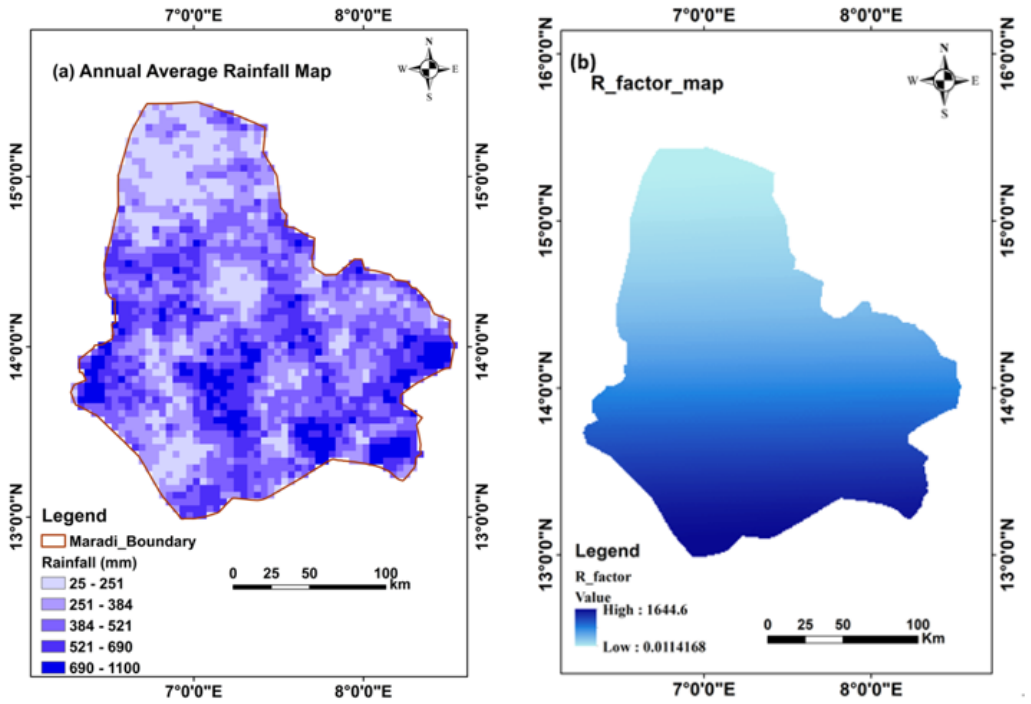

Figure 3. Map of mean annual rainfall (**a**) and distribution of rainfall erosivity (R-factor) (**b**) of the study area.

Soil erodibility (K-factor): depending on the soil texture, the K-factor reflects the cumulative effects of the soil properties. However, it shows that a particular soil type is generally resistant to erosion. The soil erodibility factor (K) was determined using the relationship proposed by Wischmeier et al. (1971) [68] (Figure 4b). Moreover, the value of the K element is influenced by the penetration potential of the soil. The spatial distribution of the K factor for the study area showed that soils with higher K values were more susceptible to soil erosion. Although, lower K values were less susceptible to soil erosion [59], ranging from 0.016 t ha h/ha MJ mm to 0.027 t ha h/ha MJ mm, indicating low to moderate soil erodibility.

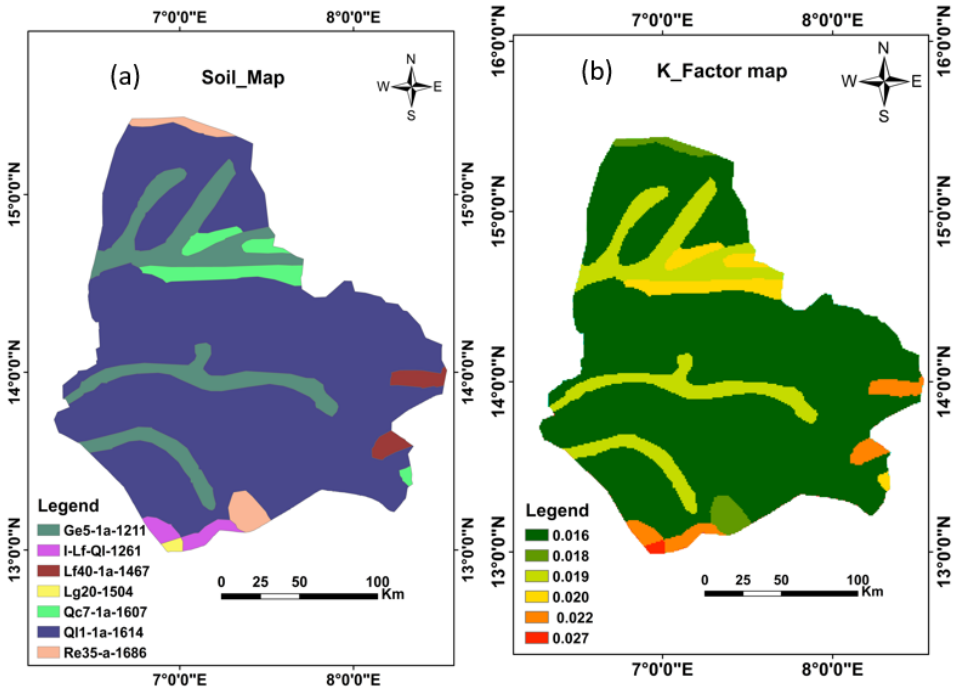

Figure 4. (**a**) Soil type and (**b**) soil erodibility (K-factor) maps.

Slope length and steepness (LS-factor): the LS-factor is used to describe the influence of the topographic component on soil erosion. It considers the topographic aspect of a particular area for soil erosion. Here, the topographic aspect represents the susceptibility of the study area to topographic erosion. It represents the influence of slope length and steepness of the slope on the mechanism of erosion (Figure 5b). River accumulation and percentage slope were used as inputs for estimating the topographic component. In the central and southern parts of the study area, the slope is high. Moreover, the slope maps identify areas with a high potential runoff and, therefore, high erosion rate; these potentials reduce as the slope degree drops from a high to a low slope degree (Figure 5a). Furthermore, the LS-factor ranged from 0 (lower part) to 111.565 (upper part). Higher LS-factor values prevailed in the central and eastern parts of the study area. The phenomenon indicates that the soil loss will increase with slope length and slope steepness. Soil loss increases faster with slope length than with slope steepness. A holistic analysis of all soil loss factors revealed that LS-factor has a significant effect on the estimation of total soil loss in the study area.

Land cover management (C-factor): the results of available vegetation cover for all land areas in the RUSLE model are numerically expressed by the C-factor, whether in agriculture or soil erosion mitigation measures. For the other main land uses in the LULC, bars were established in the area: shrublands, grasslands, croplands, urban and built-up, and forest, using the algorithm with the highest probability (Figure 6a). In the eastern and northern parts of the study area, the C-factor values were lower and the ground area was characterized by trees. However, in the southern and western parts of the zone, where a large area is characterized by bare soil and built-up areas, the C-factor values were higher. Therefore, a C-factor grid map was prepared using the LULC, and the corresponding C-factor values are shown in Figure 6b.

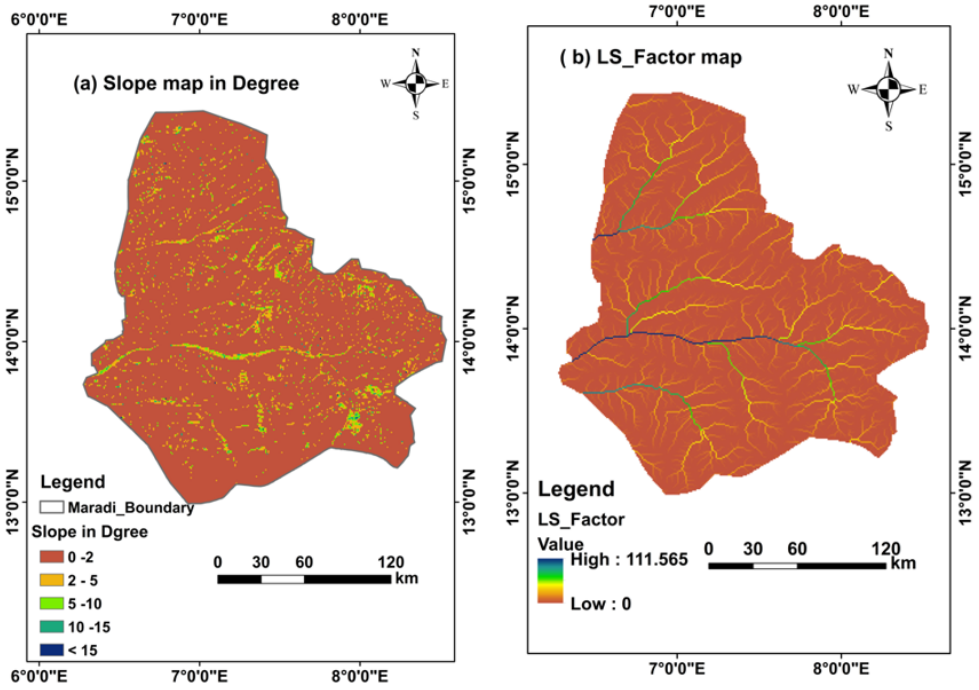

Figure 5. Slope map (**a**) and slope length and steepness (LS-factors) (**b**).

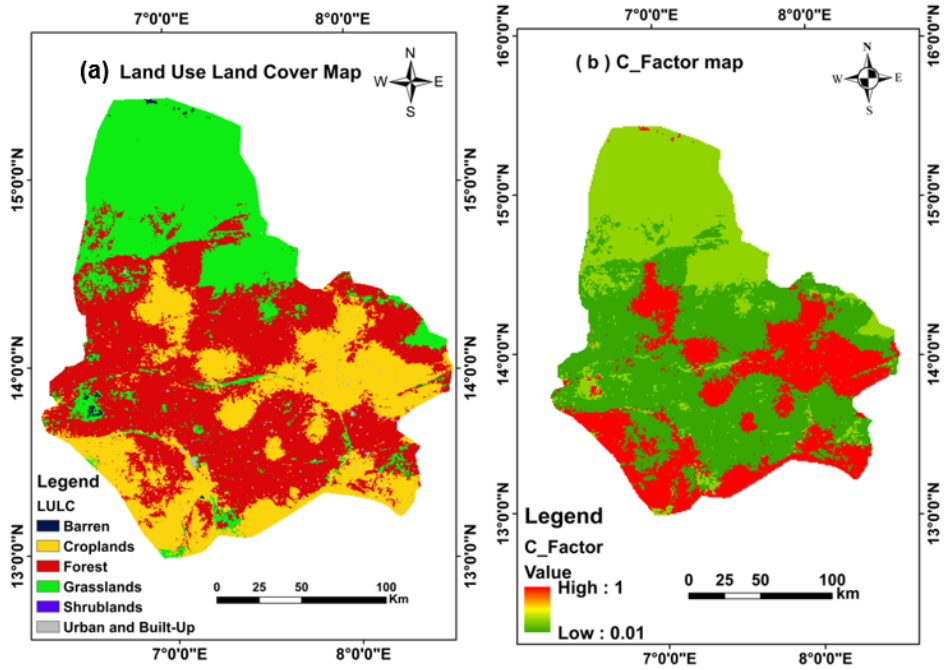

Figure 6. (**a**) Land use/land cover map and (**b**) land cover management (C-factor) map.

Conservation practices (P-factor): based on the current land management practices used in the south Central Niger, the P-factor value varied from 0.5 to 1 (Figure 7). Thus, 0.5 represents a very strong facility for protection against human erosion and 1 represents no facility for protection against human erosion [69,70]. Based on the results, lower P-factor values characterized the core area of the study zone, and higher P-factors characterized the upper part of the study area. In addition, the relevance of conservation measures increased soil erosion vulnerability. In the study area, the lower P-factor values were concentrated in the southern part of the study area, and the higher P-factor values were distributed in the upper and outer parts of the area.

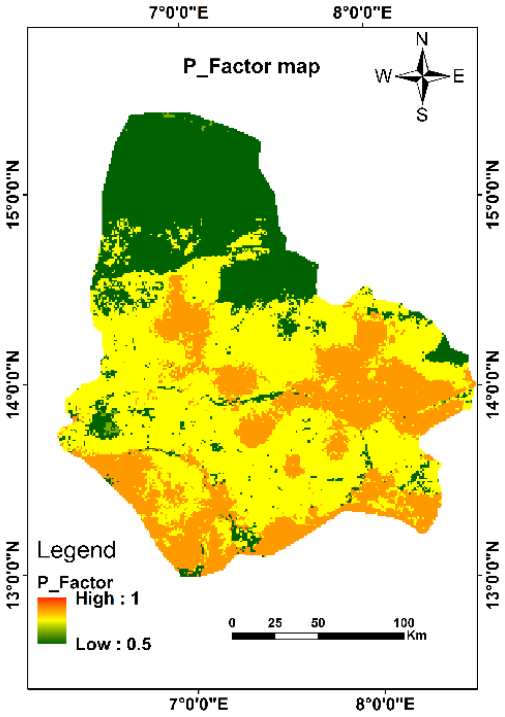

Figure 7. The conservation practice (P-factor).

3.2. Estimation of Potential Soil Erosion

For the research region, GIS, RS, and erosion models were merged to assess erosion amplitude and spatial distribution. Rainfall erosivity, soil erodibility, slope length and steepness, land cover management, and soil conservation were all identified as potential erosion factors. Figures 3–7 demonstrate the outcomes of the modelling of these variables.

It is clear from the modelling of rainfall erosivity, that (as shown in Figure 3) the stronger and longer a rainstorm lasts, the larger its erosion potential. Modeling the length and steepness of the slope yielded the results shown in Figure 5. The greater slope there is, the more runoff there will be in the long term. It is clear from Figure 5a that as the slope increases, so do the runoff velocities that cause erosion. This was confirmed by Wischmeier and Smith [69]. This component was also modelled, with the results presented in Figure 6, which shows how this affected land cover. According to the findings, plant cover has an effect on erosion because it intercepts rainwater, lowering its energy and boosting rainfall penetration.

Figure 4b shows the soil erodibility factor, which takes into account both soil erosion susceptibility and runoff volume and rate. Therefore, this illustrates how much the soil changes per unit of applied external force of energy, depending on whether water splashes or surface flows detach it.

As a result of the final soil loss model, Figure 8 shows the annual erosion map of the study area, which helps to identify the areas prone to soil erosion. This finding was supported by data from field studies in our regions with a similar environmental condition [71], where there is a high level of erosion that affects the soil and this many detrimental effects due to downstream sedimentation.

Table 4 depicts the erosion susceptibility based on LULC and slope categories, in addition to the five erosion factors that were modelled. The RUSLE model estimated yearly soil loss in the study region at 944.9 t/year, which is clearly seen in the findings (Figure 8). There was potential soil loss in the five classes, ranging from 14.8 to 944.9 t/ac/year. About 12.5% of this region's land has been lost to erosion, or 472.4 t/ac/year.

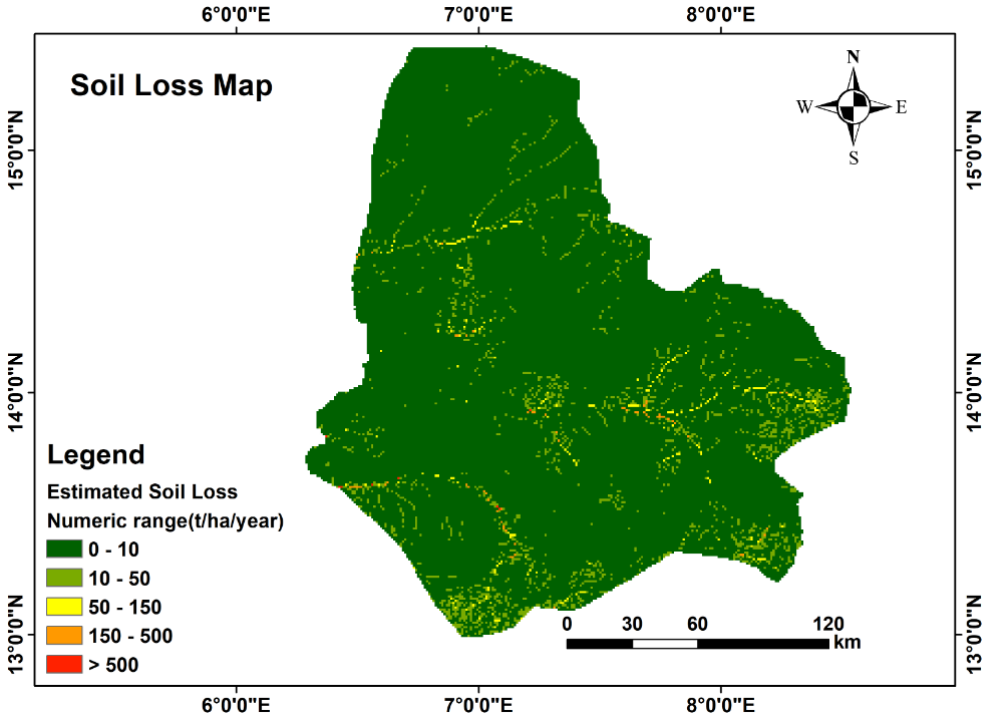

Figure 8. The potential soil erosion map of the study area.

Table 4. Soil erosion classes and range of the study area.

No	Erosion Classes	Numeric Range (t/ha/year)	Soil Loss (t/year)
1	Low	0–10	14.8
2	Moderate	10–50	85.2
3	High	50–150	237.1
4	Very High	150–500	533.5
5	Severe	>500	944.9

This explains why the land is so resistant to erosion. There is additional evidence to suggest that steep slopes erode at a considerably greater rate than level areas. As can be seen, the average rate of soil loss and the contribution to total soil loss on steeper slopes are much greater than on mild slopes.

Figure 8 shows the findings, which show that the soil erosion was minimal in all LULC classes. However, even in the somewhat forested areas, there are signs of significant erosion. Visual evaluation of the different components revealed that this was related to the high erodibility of the soil group that crosses the moderate forest LULC Class sections. There is also a considerable probability of excessive erosion in the moderate forest cover class, since it is located in the research area's heavy rainfall zones. Table 4 shows the soil erosion classes and range of the study area.

4. Conclusions and Recommendations

This paper demonstrates the use of an empirical soil erosion model such as RUSLE in conjunction with RS and GIS technology to estimate the soil erosion potential and potential zones in the Maradi region. Additionally, an effort was made to investigate the effect of changing land use/land cover on erosion rate. The analysis and results indicate that the annual average soil loss in the study area was estimated at 944.9 t/year when the RUSLE model was used. Additionally, it was observed that the amount of erosion varies significantly, according to the topography and land use/land cover.

Furthermore, the results show that slope length, steepness, and the rainfall erosivity component were the most significant variables in preventing soil erosion. The climate component was often very effective in spatial soil erosion and is a major element in climatic conditions in the RUSLE model of rainfall erosivity. Overall, areas with natural forest cover in the headwater regions had the lowest rate of soil erosion, at 14.82 t/year, whereas places with human intervention had the greatest rate, at 944.9 t/year. The highest probability approach detected shrublands, grasslands, croplands, urban and built-up, and forest areas in the study area. From 14.8 to 944.9 t/ac/year, the five classes had potential soil loss. The mean soil loss in the research region was 472.4 t/ac/year, which represents 12.5 percent of the entire area of this most eroded part. This research highlights the use of RS and GIS in evaluating soil erosion and assisting with erosion loss estimates.

Furthermore, high and severe erosion were mostly identified in high slope gradient zones and intermediate forest LULC areas. The findings showed that sites in the moderate forest LULC class had significant erosion potential, due to an intersecting high erodibility soil group. Since vegetation is a key component in soil erosion, future studies should use MODIS MCD12Q1 images obtained from more recent high-resolution satellite imagery. This will increase the accuracy of the LULC maps and DEMs used to calculate land slopes. Furthermore, validating the soil erosion loss using local data helps improve the quality and accuracy of the findings.

Additional research is required to obtain the right P-factor values within the study region, to accurately assess possible soil erosion. Overall, the findings of this research can assist in conducting proper erosion control measures in the seriously impacted areas. The data collected from this research may help in establishing management scenarios and give alternatives to policy makers for controlling soil erosion threats in the most effective way.

Author Contributions: Formal analysis, M.A.S.A. and Investigation, M.A.S.A. Methodology, Y.W., M.A.S.A., F.Z and J.F.D. Project administration, Y.W.; Supervision, Y.W. and F.Z.; Writing Original draft M.A.S.A. All authors contributed to research design, data interpretation, the literature search, and to writing the manuscript. All authors have read and agreed to the published version of the manuscript.

Funding: This study was funded by the Technology Innovation Center for Land Engineering and Human Settlements, Shaanxi Land Engineering Construction Group Co. Ltd. and Xi'an Jiaotong University (201912131-B2), the Key laboratory of Degraded and Unused Land Consolidation Engineering of Natural Resources Ministry of China (SXDJ2019-5), and Ministry of Science and Technology of the People's Republic of China (2013FY112500).

Institutional Review Board Statement: Not applicable.

Informed Consent Statement: Not applicable.

Data Availability Statement: The data supporting our analyses can be accessed publicly from the links provided in the paper, and we will also share the data soon after the manuscript is published.

Acknowledgments: We thank the Chinese Scholarship Council for financial support. We are also grateful to the editors and anonymous reviewers for their valuable time and helpful comments and suggestions.

Conflicts of Interest: The authors declare no conflict of interest.

References

1. Huang, X.; Liu, J.; Zhang, Z.; Fang, G.; Chen, Y. Assess River Embankment Impact on Hydrologic Alterations and Floodplain Vegetation. *Ecol. Indic.* **2019**, *97*, 372–379. [CrossRef]
2. Maqsoom, A.; Aslam, B.; Hassan, U.; Kazmi, Z.A.; Sodangi, M.; Tufail, R.F.; Farooq, D. Geospatial Assessment of Soil Erosion Intensity and Sediment Yield Using the Revised Universal Soil Loss Equation (RUSLE) Model. *ISPRS Int. J. Geo-Inf.* **2020**, *9*, 356. [CrossRef]
3. Ping, Z.; Yajin, G.E.; JIANG, Y.; Yanan, X.I.E.; Zhiwen, S.I.; Hainan, Y.; Hong-Yuan, H.U.O.; Junchuan, Y.U.; Guanyuan, W.E.I. Assessment of Soil Erosion by the RUSLE Model Using Remote Sensing and GIS: A Case Study of Jilin Province of China. *Preprints* **2020**. [CrossRef]

4. Sun, L.; Wan, S.; Luo, W. Biochars Prepared from Anaerobic Digestion Residue, Palm Bark, and Eucalyptus for Adsorption of Cationic Methylene Blue Dye: Characterization, Equilibrium, and Kinetic Studies. *Bioresour. Technol.* **2013**, *140*, 406–413. [CrossRef]
5. Gao, J. Wetland and Its Degradation in the Yellow River Source Zone. In *Landscape and Ecosystem Diversity, Dynamics and Management in the Yellow River Source Zone*; Springer: Berlin, Germany, 2016; pp. 209–232.
6. Boakye, E.; Anyemedu, F.O.K.; Donkor, E.A.; Quaye-Ballard, J.A. Spatial Distribution of Soil Erosion and Sediment Yield in the Pra River Basin. *SN Appl. Sci.* **2020**, *2*, 320. [CrossRef]
7. Grepperud, S. Soil Conservation and Governmental Policies in Tropical Areas: Does Aid Worsen the Incentives for Arresting Erosion? *Agric. Econ. J. Int. Assoc. Agric. Econ.* **1995**, *12*, 129–140.
8. Dabral, P.P.; Baithuri, N.; Pandey, A. Soil Erosion Assessment in a Hilly Catchment of North Eastern India Using USLE, GIS and Remote Sensing. *Water Resour Manag.* **2008**, *22*, 1783–1798. [CrossRef]
9. Latrubesse, E.M.; Arima, E.Y.; Dunne, T.; Park, E.; Baker, V.R.; d'Horta, F.M.; Wight, C.; Wittmann, F.; Zuanon, J.; Baker, P.A.; et al. Damming the Rivers of the Amazon Basin. *Nature* **2017**, *546*, 363–369. [CrossRef]
10. Wiedmann, T.; Lenzen, M.; Keyßer, L.T.; Steinberger, J.K. Scientists' Warning on Affluence. *Nat. Commun.* **2020**, *11*, 3107. [CrossRef]
11. Hoyos, N. Spatial Modeling of Soil Erosion Potential in a Tropical Watershed of the Colombian Andes. *Catena* **2005**, *63*, 85–108. [CrossRef]
12. Pandey, A.; Mathur, A.; Mishra, S.K.; Mal, B.C. Soil Erosion Modeling of a Himalayan Watershed Using RS and GIS. *Env. Earth Sci.* **2009**, *59*, 399–410. [CrossRef]
13. Prasannakumar, V.; Vijith, H.; Abinod, S.; Geetha, N. Estimation of Soil Erosion Risk within a Small Mountainous Sub-Watershed in Kerala, India, Using Revised Universal Soil Loss Equation (RUSLE) and Geo-Information Technology. *Geosci. Front.* **2012**, *3*, 209–215. [CrossRef]
14. Ullah, S.; Ali, A.; Iqbal, M.; Javid, M.; Imran, M. Geospatial Assessment of Soil Erosion Intensity and Sediment Yield: A Case Study of Potohar Region, Pakistan. *Environ. Earth Sci.* **2018**, *77*, 705. [CrossRef]
15. Zhao, F.; Wu, Y.; Qiu, L.; Sun, Y.; Sun, L.; Li, Q.; Niu, J.; Wang, G. Parameter Uncertainty Analysis of the SWAT Model in a Mountain-Loess Transitional Watershed on the Chinese Loess Plateau. *Water* **2018**, *10*, 690. [CrossRef]
16. Sidi Almouctar, M.A.; Wu, Y.; Kumar, A.; Zhao, F.; Mambu, K.J.; Sadek, M. Spatiotemporal Analysis of Vegetation Cover Changes around Surface Water Based on NDVI: A Case Study in Korama Basin, Southern Zinder, Niger. *Appl. Water Sci.* **2020**, *11*, 4. [CrossRef]
17. Fagbohun, B.J.; Anifowose, A.Y.B.; Odeyemi, C.; Aladejana, O.O.; Aladeboyeje, A.I. GIS-Based Estimation of Soil Erosion Rates and Identification of Critical Areas in Anambra Sub-Basin, Nigeria. *Model. Earth Syst. Environ.* **2016**, *2*, 159. [CrossRef]
18. Adediji, A.; Tukur, A.M.; Adepoju, K.A. Assessment of Revised Universal Soil Loss Equation (RUSLE) in Katsina Area, Katsina State of Nigeria Using Remote Sensing (RS) and Geographic Information System (GIS). *Iran. J. Energy Environ.* **2010**, *1*, 255–264.
19. Mhangara, P.; Kakembo, V.; Lim, K.J. Soil Erosion Risk Assessment of the Keiskamma Catchment, South Africa Using GIS and Remote Sensing. *Environ. Earth Sci.* **2012**, *65*, 2087–2102. [CrossRef]
20. Ravi, K.K.; Asadi, S.S.; Venkata Ratnam, K. Estimation of Soil Erosion Status for Land Resources Management Using Remote Sensing and GIS: A Model Study from A.P. *Int. J. Mech. Eng. Technol.* **2017**, *8*, 873–880.
21. Atoma, H.; Suryabhagavan, K.V.; Balakrishnan, M. Soil Erosion Assessment Using RUSLE Model and GIS in Huluka Watershed, Central Ethiopia. *Sustain. Water Resour. Manag.* **2020**, *6*, 12. [CrossRef]
22. Hurni, H. Land Degradation, Famine and Resource Scenarios in Ethiopia. In *World Soil Erosion and Conservation*; Pimentel, D., Ed.; Cambridge University Press: Cambridge, UK, 1993; pp. 27–62. [CrossRef]
23. Maina, C.W.; Sang, J.K.; Raude, J.M.; Mutua, B.M.; Moriasi, D.N. Sediment Distribution and Accumulation in Lake Naivasha, Kenya over the Past 50 Years. *Lakes Amp. Reserv.* **2019**, *24*, 162–172. [CrossRef]
24. Iradukunda, P.; Bwambale, E. Reservoir Sedimentation and Its Effect on Storage Capacity–A Case Study of Murera Reservoir, Kenya. *Cogent Eng.* **2021**, *8*, 1917329. [CrossRef]
25. Kastridis, A.; Kamperidou, V. Influence of Land Use Changes on Alleviation of Volvi Lake Wetland (North Greece). *Soil Water Res.* **2016**, *10*, 121–129. [CrossRef]
26. Parveen, R.; Kumar, U. Integrated Approach of Universal Soil Loss Equation (USLE) and Geographical Information System (GIS) for Soil Loss Risk Assessment in Upper South Koel Basin, Jharkhand. *J. Geogr. Inf. Syst.* **2012**, *4*, 588–596. [CrossRef]
27. Yeshaneh, G.T. Assessment of Soil Fertility Variation in Different Land Uses and Management Practices in Maybar Watershed, South Wollo Zone, North Ethiopia. *Int. J. Environ. Bioremedi. Biodegrad.* **2015**, *3*, 15–22.
28. Chen, S.; Zha, X. Evaluation of Soil Erosion Vulnerability in the Zhuxi Watershed, Fujian Province, China. *Nat. Hazards* **2016**, *82*, 1589–1607. [CrossRef]
29. Molla, T.; Sisheber, B. Estimating Soil Erosion Risk and Evaluating Erosion Control Measures for Soil Conservation Planning at Koga Watershed in the Highlands of Ethiopia. *Solid Earth* **2017**, *8*, 13. [CrossRef]
30. Wynants, M.; Kelly, C.; Mtei, K.; Munishi, L.; Patrick, A.; Rabinovich, A.; Nasseri, M.; Gilvear, D.; Roberts, C.N.; Boeckx, P. Drivers of Increased Soil Erosion in East Africa's Agro-Pastoral Systems: Changing Interactions between the Social, Economic and Natural Domains. *Reg. Environ. Chang.* **2019**, *19*, 1909–1921. [CrossRef]

31. Brath, A.; Castellarin, A.; Montanari, A. Assessing the Effects of Land-Use Changes on Annual Average Gross Erosion. *Hydrol. Earth Syst. Sci.* **2002**, *6*, 255–265. [CrossRef]
32. Ganasri, B.P.; Ramesh, H. Assessment of Soil Erosion by RUSLE Model Using Remote Sensing and GIS - A Case Study of Nethravathi Basin. *Geosci. Front.* **2016**, *7*, 953–961. [CrossRef]
33. Fu, B.; Wang, S.; Liu, Y.; Liu, J.; Liang, W.; Miao, C. Hydrogeomorphic Ecosystem Responses to Natural and Anthropogenic Changes in the Loess Plateau of China. *Annu. Rev. Earth Planet. Sci.* **2017**, *45*, 223–243. [CrossRef]
34. Tadesse, L.; Suryabhagavan, K.V.; Sridhar, G.; Legesse, G. Land Use and Land Cover Changes and Soil Erosion in Yezat Watershed, North Western Ethiopia. *Int. Soil Water Conserv. Res.* **2017**, *5*, 85–94. [CrossRef]
35. El Jazouli, A.; Barakat, A.; Khellouk, R.; Rais, J.; El Baghdadi, M. Remote Sensing and GIS Techniques for Prediction of Land Use Land Cover Change Effects on Soil Erosion in the High Basin of the Oum Er Rbia River (Morocco). *Remote. Sens. Appl. Soc. Environ.* **2019**, *13*, 361–374. [CrossRef]
36. Renard, K.G.; Foster, G.R.; Weesies, G.A.; McCool, D.K.; Yoder, D.C. *Predicting Soil Erosion by Water: A Guide to Conservation Planning with the Revised Universal Soil Loss Equation (RUSLE)*; United States Government Printing: Washington, DC, USA, 1997.
37. Kefi, M.; Yoshino, K.; City, T. Evaluation of the Economic Effects of Soil Erosion Risk on Agricultural Productivity Using Remote Sensing: Case of Watershed in Tunisia. *Int. Arch. Photogramm. Remote. Sens. Spat. Inf. Sci.* **2010**, *38*, 930.
38. Yoshino, K.; Ishioka, Y. Guidelines for Soil Conservation towards Integrated Basin Management for Sustainable Development: A New Approach Based on the Assessment of Soil Loss Risk Using Remote Sensing and GIS. *Paddy Water Env.* **2005**, *3*, 235–247. [CrossRef]
39. Hacısalihoglu, S.; Oktan, E.; Yucesan, Z. Predicting Soil Erosion in Oriental Spruce (Picea Orientalis (L.) Link.) Stands in Eastern Black Sea Region of Turkey. *Afr. J. Agric. Res.* **2010**, *5*, 2200–2214.
40. Leh, M.; Bajwa, S.; Chaubey, I. Impact of Land Use Change on Erosion Risk: An Integrated Remote Sensing, Geographic Information System and Modeling Methodology. *Land Degrad. Dev.* **2013**, *24*, 409–421. [CrossRef]
41. Kefi, M.; Yoshino, K.; Zayani, K.; Isoda, H. Estimation of Soil Loss by Using Combination of Erosion Model and GIS. *Case Study Watersheds Tunis. J. Arid Land Stud.* **2009**, *19*, 287–290.
42. Anache, J.A.A.; Bacchi, C.G.V.; Panachuki, E.; Sobrinho, T.A. Assessment of Methods for Predicting Soil Erodibility in Soil Loss Modeling. *Geociências* **2016**, *34*, 32–40.
43. Chappell, A.; Warren, A.; Taylor, N.; Charlton, M. Soil flux (loss and gain) in southwestern Niger and its agricultural impact. *Land Degrad. Dev.* **1998**, *9*, 295–310. [CrossRef]
44. Panagos, P.; Meusburger, K.; Alewell, C.; Montanarella, L. Soil Erodibility Estimation Using LUCAS Point Survey Data of Europe. *Environ. Model. Softw.* **2012**, *30*, 143–145. [CrossRef]
45. Bonilla, C.A.; Johnson, O.I. Soil Erodibility Mapping and Its Correlation with Soil Properties in Central Chile. *Geoderma* **2012**, *189*, 116–123. [CrossRef]
46. Boggs, G.; Devonport, C.; Evans, K.; Puig, P. GIS-Based Rapid Assessment of Erosion Risk in a Small Catchment in the Wet/Dry Tropics of Australia. *Land Degrad. Dev.* **2001**, *12*, 417–434. [CrossRef]
47. Van Remortel, R.D.; Hamilton, M.E.; Hickey, R.J. Estimating the LS Factor for RUSLE through Iterative Slope Length Processing of Digital Elevation Data within Arclnfo Grid. *Cartography* **2001**, *30*, 27–35. [CrossRef]
48. Fan, J.R.; Zhang, J.H.; Zhong, X.H.; Liu, S.Z.; Tao, H.P. Monitoring of Soil Erosion and Assessment for Contribution of Sediments to Rivers in a Typical Watershed of the Upper Yangtze River Basin. *Land Degrad. Dev.* **2004**, *15*, 411–421. [CrossRef]
49. Tian, Y.C.; Zhou, Y.M.; Wu, B.F.; Zhou, W.F. Risk Assessment of Water Soil Erosion in Upper Basin of Miyun Reservoir, Beijing, China. *Env. Geol.* **2009**, *57*, 937–942. [CrossRef]
50. Tzioutzios, C.; Kastridis, A. Multi-Criteria Evaluation (MCE) Method for the Management of Woodland Plantations in Floodplain Areas. *Int. J. Geo-Inf.* **2020**, *9*, 725. [CrossRef]
51. Pangali Sharma, T.P.; Zhang, J.; Khanal, N.R.; Prodhan, F.A.; Nanzad, L.; Zhang, D.; Nepal, P. A Geomorphic Approach for Identifying Flash Flood Potential Areas in the East Rapti River Basin of Nepal. *Int. J. Geo-Inf.* **2021**, *10*, 247. [CrossRef]
52. Rawat, K.S.; Mishra, A.K.; Bhattacharyya, R. Soil Erosion Risk Assessment and Spatial Mapping Using LANDSAT-7 ETM+, RUSLE, and GIS—A Case Study. *Arab. J. Geosci.* **2016**, *9*, 288. [CrossRef]
53. Alhassane, A.; Chaibou, I.; Karim, S.; Soumana, I.; Mahamane, A.; Saadou, M. Flore et Structure Des Peuplements Ligneux Des Pâturages Naturels de La Région de Maradi, Niger. *Afr. Sci.* **2018**, *14*, 171–189.
54. Download Data by Country | DIVA-GIS. Available online: https://www.diva-gis.org/gdata (accessed on 27 September 2021).
55. FAO. Digital Soil Map of the World (DSMW) | Land & Water | Food and Agriculture Organization of the United Nations Land & Water | Food and Agriculture Organization of the United Nations. Available online: http://www.fao.org/land-water/land/land-governance/land-resources-planning-toolbox/category/details/en/c/1026564/ (accessed on 20 September 2021).
56. USGS-EarthExplorer. Available online: https://earthexplorer.usgs.gov/ (accessed on 20 September 2021).
57. Simpson, J.; Kummerow, C.; Tao, W.K.; Adler, R.F. On the tropical rainfall measuring mission (TRMM). *Meteorol. Atmos. Phys.* **1996**, *60*, 19–36. [CrossRef]
58. Biswas, S.S.; Pani, P. Estimation of Soil Erosion Using RUSLE and GIS Techniques: A Case Study of Barakar River Basin, Jharkhand, India. *Modeling Earth Syst. Environ.* **2015**, *4*, 42. [CrossRef]
59. Thapa, P. Spatial Estimation of Soil Erosion Using RUSLE Modeling: A Case Study of Dolakha District, Nepal. *Env. Syst. Res.* **2020**, *9*, 15. [CrossRef]

60. Wang, B.; Zheng, F.; Guan, Y. Improved USLE-K Factor Prediction: A Case Study on Water Erosion Areas in China. *Int. Soil Water Conserv. Res.* **2016**, *4*, 168–176. [CrossRef]
61. Belayneh, M.; Yirgu, T.; Tsegaye, D. Potential Soil Erosion Estimation and Area Prioritization for Better Conservation Planning in Gumara Watershed Using RUSLE and GIS Techniques'. *Environ. Syst. Res.* **2019**, *8*, 20. [CrossRef]
62. Farhan, Y.; Nawaiseh, S. Spatial Assessment of Soil Erosion Risk Using RUSLE and GIS Techniques. *Environ. Earth Sci.* **2015**, *74*, 4649–4669. [CrossRef]
63. Diwediga, B.; Le, Q.B.; Agodzo, S.K.; Tamene, L.D.; Wala, K. Modelling Soil Erosion Response to Sustainable Landscape Management Scenarios in the Mo River Basin (Togo, West Africa). *Sci. Total. Environ.* **2018**, *625*, 1309–1320. [CrossRef]
64. Alewell, C.; Borrelli, P.; Meusburger, K.; Panagos, P. Using the USLE: Chances, Challenges and Limitations of Soil Erosion Modelling. *Int. Soil Water Conserv. Res.* **2019**, *7*, 203–225. [CrossRef]
65. Yesuph, A.Y.; Dagnew, A.B. Soil Erosion Mapping and Severity Analysis Based on RUSLE Model and Local Perception in the Beshillo Catchment of the Blue Nile Basin, Ethiopia. *Environ. Syst. Res.* **2019**, *8*, 17. [CrossRef]
66. Wischmeier, W.H.; Johnson, C.B.; Cross, B.V. Soil Erodibility Nomograph for Farmland and Construction Sites. *J. Soil Water Conserv.* **1971**. Available online: https://trid.trb.org/view/125184 (accessed on 30 November 2021).
67. Obiora-Okeke, O.A. Erosion mapping using revised universal soil loss equation model and geographic information system: A case study of Okitipupa, Nigeria. *Eur. J. Eng. Technol.* **2019**, *7*. Available online: https://www.idpublications.org/wp-content/uploads/2019/05/Full-Paper-EROSION-MAPPING-USING-REVISED-UNIVERSAL-SOIL-LOSS-EQUATION-MODEL-AND-GEOGRAPHIC-INFORMATION.pdf (accessed on 30 November 2021).
68. Olorunfemi, I.E.; Komolafe, A.A.; Fasinmirin, J.T.; Olufayo, A.A.; Akande, S.O. A GIS-Based Assessment of the Potential Soil Erosion and Flood Hazard Zones in Ekiti State, Southwestern Nigeria Using Integrated RUSLE and HAND Models. *Catena* **2020**, *194*, 104725. [CrossRef]
69. Wischmeier, W.H.; Smith, D.D. *Predicting Rainfall Erosion Losses: A Guide to Conservation Planning*; Department of Agriculture, Science and Education Administration: Corvallis, OR, USA, 1978.
70. Ekwueme, O.U.; Obiora, D.N.; Okeke, F.N.; Ibuot, C. Environmental Assessment of Gully Erosion in Parts of Enugu North, Southeastern Nigeria. *Indian J. Sci. Technol.* **2021**, *14*, 2400–2409. [CrossRef]
71. Uddin, K.; Murthy, M.S.R.; Wahid, S.M.; Matin, M.A. Estimation of Soil Erosion Dynamics in the Koshi Basin Using GIS and Remote Sensing to Assess Priority Areas for Conservation. *PLoS ONE* **2016**, *11*, e0150494. [CrossRef] [PubMed]